

Critical behavior of strained epitaxial Gd films: *In situ* ac-susceptibility measurements in UHV

U. Stetter, M. Farle,* and K. Baberschke

Institut für Experimentalphysik, Freie Universität Berlin, Arnimallee 14, D-1000 Berlin 33, Germany

W. G. Clark

Department of Physics, University of California, Los Angeles, California 90024-1547

(Received 21 August 1991)

300-Å Gd films grown on W(110) under UHV conditions have been investigated *in situ* by ac-susceptibility measurements above and below T_c . A sharp peak of $\chi_{ac}=230$ is observed. To our knowledge, this is the largest and sharpest ($2\sigma=1$ K) cusp measured for a rare-earth ferromagnet. No domain-wall signal is superimposed upon the divergence of the paramagnetic susceptibility. At T_c^+ we find $\chi=\chi_0 t^{-\gamma}$ with $\gamma=1.235(25)$. This is clear evidence for a three-dimensional Ising-like behavior above T_c . The sharpness and peak position of $\chi(T)$ change, depending on the annealing temperature. Simultaneously, a change in the LEED pattern is observed.

Recently, an increasing number of reports have focused on the magnetic properties of thin films of pure metals and the dependence on their crystallographic quality.^{1,2} The misfit to the substrate, the temperature during the deposition, and annealing affect the magnetic properties.³⁻⁶ The Curie temperature depends on the thickness^{7,8} as well as on internal strain. Bulk studies^{9,10} show the effect of annealing on the sharpening of the phase transition for Gd polycrystals. In the present study we have used the thin-film ultrahigh-vacuum (UHV) technique to prepare almost perfect metallic rare-earth films of thickness 300 Å. The *in situ* measurement of the ac susceptibility allows us to follow the change in the magnetism near the phase transition as a function of the structural behavior in a controlled and reproducible way.

Our 300-Å-thick Gd thin films are deposited onto a clean W(110) disk at $p < 2 \times 10^{-10}$ mbar during evaporation. The film growth is monitored by Auger-electron spectroscopy (AES) and low-energy electron diffraction (LEED). In contrast to our earlier works,^{8,11} the substrate is held at room temperature. This results in a layer by layer growth¹² of the first few layers. Gd grows with the hexagonal basal plane parallel to the surface. The lattice mismatch along the [100] direction of the bcc W(110) surface is approximately 15%. This large mismatch results in a 4.4% compression of the first Gd layer.¹² The corresponding strain causes many dislocations in the second and the following layers. In the elastic-continuum theory, one estimates that the critical thickness is $h_c = 2$ Å for the nucleation of misfit dislocations. This means that the strained lattice of Gd relaxes by incorporating dislocations from the second layer on.¹³ Such a structure yields diffuse LEED patterns, which we observe for the freshly deposited film. After deposition to the desired thickness, the films are annealed *in situ* in steps of about 50 K. Already after the second annealing step (395 K), distinct spots of the hexagonal Gd pattern appear. They become sharper until the film has relaxed completely at ≈ 870 K. That means the surface has become laterally homogeneous at least over the coherence length (> 100 Å) of LEED. In the same way the misfit

dislocations are annealed out, and the magnetic properties of the film become more ideal. This simultaneous and *in situ* observation of structural and magnetic properties is demonstrated in the present investigation. Only on well-ordered films one can study the critical behavior.

Figure 1 shows some spectra of the real part of the ac susceptibility χ_{ac} recorded over a temperature range of 80 K for several annealing steps. The Curie-Weiss peak in the temperature-dependent susceptibility at T_c , which is smeared out for the freshly deposited film, narrows considerably upon annealing. Simultaneously the maximum of the susceptibility of the film annealed at 328 K shifts to 292.1(5) K after successive annealing (5 min) in steps up to 870 K. Short annealing at higher temperatures does not produce any further changes. The measured Curie temperature of the annealed 300-Å film agrees with the

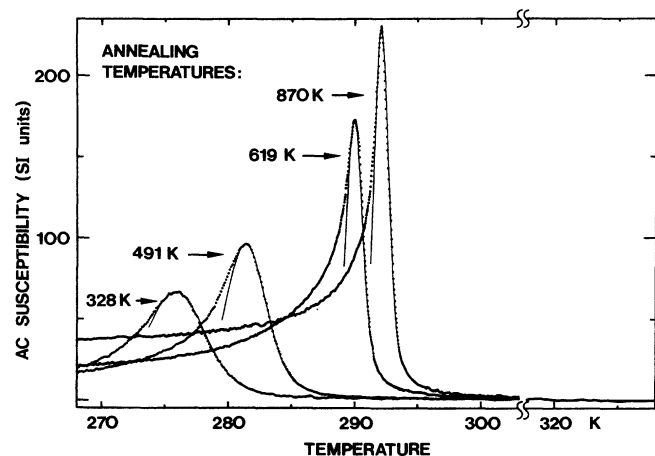


FIG. 1. ac susceptibility close to T_c of the 300-Å thin-film Gd(0001)/W(110) for several annealing steps. The solid lines are simulations using Eq. (4). Note that in bulk ferromagnets (Ref. 17) and in imperfect films (Refs. 15, 16, and 18), the domain-wall response dominates over the paramagnetic signal and affects the analysis with Eq. (2). The error for χ_{ac} is $\pm 5\%$.

bulk Gd values published so far (Table 1 in Ref. 10). The sample temperature is measured by a W/Re thermocouple (relative sensitivity 0.03 K). The calibration is accurate to ± 0.5 K. The ac susceptibility is measured with a trimmed mutual-induction bridge.¹⁴ For technical details, see Ref. 15. The signal is calibrated with the known susceptibility of Gd sulfate in *Système International* units. The low primary ac field (182 Hz, $H_{\text{rms}} = 50$ A/m) oscillates in the film plane.

The observed peak at T_c of the best film is much sharper than previously reported in the literature for pure Gd metal. The following four reasons give an explanation.

(i) For Gd the high reaction enthalpy with oxygen and hydrogen causes problems of sample contamination. The use of the ultraclean UHV technique avoids this problem. It is not surprising that a Gd film contaminated in air shows a reduced signal,¹⁶ because the chemisorbed atoms disturb the lattice structure of the surface and therefore the magnetism. For example, the peak in the susceptibility of our annealed 300-Å film is reduced by a factor of 4 after exposing to air.

(ii) Dislocations, lattice defects, and locally varying strains restrict the divergence of the coherence length at T_c in any real sample. This cluster-size effect influences the ordering temperature. Thus, one usually measures a distribution of Curie temperatures averaged over the sample. That broadens the susceptibility peak, as seen in Fig. 1 for the nonannealed film. Clusters with a randomly oriented magnetization below T_c correlate at much lower temperatures and exhibit superparamagnetism. This leads to a slowly increasing susceptibility with decreasing temperature as shown in Ref. 17.

(iii) The curves in Fig. 1 exhibit the initial susceptibility of nearly the ideal paramagnetic χ_{para} . The ferromagnetic contribution χ_{wall} of the domain-wall response is negligible in an almost perfect film with very few domains.

(iv) Our measurements are taken with the drive field parallel to the film plane to minimize the demagnetizing factor N which limits the divergence of χ_{ext} :

$$\chi_{\text{ext}} = \frac{\chi_{\text{int}}}{1 + N\chi_{\text{int}}}, \quad \lim_{\chi_{\text{int}} \rightarrow \infty} \chi_{\text{ext}} = \frac{1}{N}. \quad (1)$$

In addition to the specific heat and the spontaneous magnetization, the magnetic susceptibility is important for describing the magnetic properties of a ferromagnet. At present there is an ambiguity in the critical behavior of gadolinium. Since it is an s -state ion, Gd should be an ideal Heisenberg ferromagnet. The experimental values of the critical exponent α for the specific heat support this.¹⁹ The exponent β for the spontaneous magnetization spans both the Heisenberg-²⁰ and Ising-²¹ model predictions. The exponent γ for χ ranges between 1.18(15) (Ref. 22) and 1.25(10) (Ref. 23) in agreement with the three-dimensional (3D) Ising-model theoretical value 1.2402(9).²⁴ We analyze the critical behavior of the best Gd film above T_c in terms of the power law (2) for the initial susceptibility.

$$\chi = \chi_0^+ t^{-\gamma}, \quad (2)$$

where $t = T/T_c - 1$, and χ_0^+ denotes the critical amplitude at T_c^+ . The least-squares fit (LSF) is shown in Fig. 2.

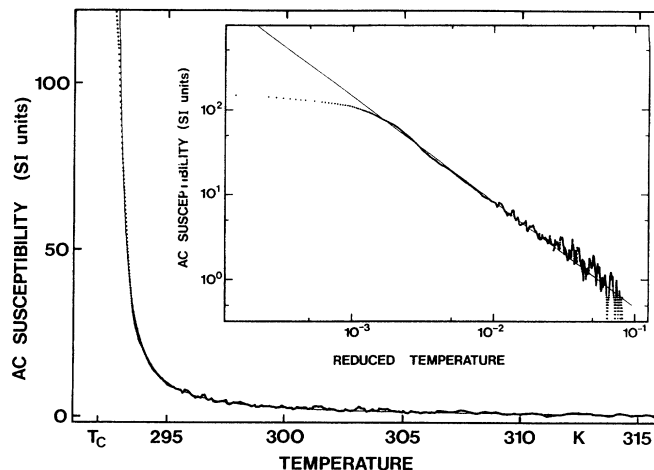


FIG. 2. Least-squares fit by a power law [Eq. (2)] of the experimental data for the best Gd film after annealing at 870 K. Both linear and logarithmic plots are shown.

We find a power law with $\gamma = 1.235(25)$ and $\chi_0^+ = 3.5(4) \times 10^{-2}$ in the temperature interval $10^{-3} < t < 10^{-1}$. This exponent value confirms our previous study on the electron-spin-resonance intensity of a 80-Å film⁸ that the paramagnetic Gd film behaves as a 3D Ising system. Geldart *et al.*²⁵ determined $\gamma = 1.23(2)$ along the c axis. But for the basal plane they fitted 1.01(3) with an offset in the signal, which they attributed to uniaxial anisotropy. However, they measured a cube-shaped single crystal with $N > \frac{1}{3}$. This limits the observable susceptibility far above T_c , resulting in deviations from the power law below $t = 10^{-2}$. Their four-parameter fits, large N , and bulk samples make the determination of γ less reliable. Furthermore, for metallic ferromagnets we see no justification for anisotropic γ values.

Previously, only Wantenaar *et al.*¹⁰ estimated roughly the magnitude of the susceptibility signal by calculating the coil-system data. They find a value for the critical amplitude $\chi_0^+ = 1.05 \times 10^{-2}$ for a Gd polycrystal torus assuming $N = 0$. The critical amplitude depends on the crystal symmetry and the type of interaction. Baker²⁶ and Ritchie and Fisher²⁷ calculated χ_0^+ in the Padé approximation for simple cubic, bcc, and fcc lattice with Ising and Heisenberg interaction, respectively:

$$\chi_0^+ = 4\pi \frac{C^+ M(0)^2}{k_B T} \frac{1}{n}, \quad (3)$$

with $C^+ = 0.85$ to 1.2. The value for hexagonal Gd has not been calculated so far. Assuming $C^+ = 1$ and using for Gd $M(0) = 0.214$ T, $n = 3.01 \times 10^{22}/\text{cm}^3$, and $T_c = 292$ K, one estimates $\chi_0^+ = 4.7 \times 10^{-2}$. The value determined from the experiment $\chi_0^+ = 3.5 \times 10^{-2}$ is in fair agreement.

Now we analyze the influence of annealing on the magnetic behavior of the Gd films. We assume the experimental susceptibility curves to be a superposition of ideal theoretical power laws (2), where T_c may vary locally due to different internal strains and finite cluster sizes. Assuming a Gaussian distribution of T_c values in Eq. (2) with a full width 2σ , we fit all experimental susceptibility

curves in Fig. 1 for each annealing step using

$$\chi_{\text{sim}} = \int_{T_c - 30\text{K}}^{T_c + 30\text{K}} \frac{\chi_0^{\pm} [(|T - T'|)/T']^{-\gamma}}{1 + N \{ \chi_0^{\pm} [(|T - T'|)/T']^{-\gamma} \}} \frac{1}{2\sigma\sqrt{\pi/2}} \times \exp\{-2[(T' - T_c)/2\sigma]^2\} dT'. \quad (4)$$

The γ above and below T_c was taken to be the 3D Ising value, $\gamma = 1.240$, and the critical amplitude $\chi_0^+ = 2\chi_0^- = 3.5 \times 10^{-2}$. For the sharpest peak the demagnetizing factor is determined to $5(2) \times 10^{-4}$ and was kept constant for the other fits. The only free fit parameters are 2σ , which varies with the annealing temperature, and T_c . Note that T_c equals the temperature where $\chi(T)$ is maximal, and is not an undefined value as in Ref. 16. The results are listed in Table I. Within experimental error, the fits in Fig. 1 agree with the data above T_c . Below T_c the deviation of the fits is due to the small contribution of the very few domain walls χ_{wall} , which vanish above T_c . This will be discussed elsewhere. In the present investigation we focus on the analysis of $\chi(T)$ at and above T_c . For this regime very small contributions of χ_{wall} can be neglected in contrast to measurements with high ac fields on polycrystalline samples.²⁸

In the previous paragraph we presented evidence that the sharp but finite width of $\chi(T)$ is due to a T_c distribution. If this spread would have been ignored, a fit to the simple equation (2) deviates from $\chi(T)$ below $t \approx 3 \times 10^{-3}$ (inset in Fig. 2). This value $t = 3 \times 10^{-3}$ equals $T_c + 2\sigma$. The recently reported crossover at $t < 10^{-3}$,²⁹ which was attributed to dipolar interactions, may well be due to sample imperfections and the resulting problems discussed above.

To explain the large Curie temperature decrease of 16 K in the nonperfect (strained) films with dislocations, we compare it with Monte Carlo simulations from Soukoulis, Grest, and Velgakis.³⁰ Their model predicts that a 5% concentration of defects in the lattice, which is consistent with a diffuse LEED pattern, leads to a lowering of the mean T_c in Gd by 15 K.

TABLE I. Results of the simulations using Eq. (4). T_{ann} is the annealing temperature as shown in Fig. 1, T_c is the Curie temperature, and 2σ is the full width of the temperature distribution (all in units of K).

T_{ann}	328	491	619	870
T_c	275.7(5)	281.3(5)	289.9(5)	292.1(5)
2σ	4.4(1)	3.0(1)	1.13(3)	1.02(2)

In summary, the present experiment shows a sharp and large peak in the paramagnetic susceptibility for elementary ferromagnetic metals. This is due to the single domain behavior and high purity (much better than bulk materials) of the films, which are prepared and measured *in situ* under UHV. In addition the demagnetizing factor of $N \approx 10^{-4}$, being much smaller than for bulk samples, enables χ_{ext} to reach larger values. This condition allows a high reliability for the determination of γ and T_c in the present and future experiments. The second important aspect of the present work lies in its future applicability to UHV surface magnetism. Until now the Curie temperatures of monolayers and multilayers of Co, Fe, etc., were determined by measurements of the direct magnetization and the asymmetry parameter in spin-polarized photoemission spectroscopy, LEED, AES, and by the Mössbauer technique. All these techniques are less reliable, since they probe $M(T)$, which is a vanishing quantity at T_c . Furthermore, the macroscopic M may be zero even for a nonvanishing order parameter. Further application of *in situ* UHV susceptibility measurements will improve our understanding of thin-film magnetism, in particular, Fig. 1 demonstrates that this technique is monolayer sensitive.

We thank Yi Li and B. Clemens for helpful discussions. This work was supported in part by Deutsche Forschungsgemeinschaft, Sonderforschungsbereich 6, TP A03.

*Present address: Department of Material Science and Engineering, Stanford University, Stanford, CA 94305-2205.

¹C. Y. Shih, C. L. Bauer, and J. O. Artman, *J. Appl. Phys.* **64**, 5428 (1988).

²D. LaGraffe, P. A. Dowben, and M. Onellion, *Phys. Rev. B* **40**, 970 (1989).

³R. Allenspach, M. Stampanoni, and A. Bischof, *Phys. Rev. Lett.* **65**, 3344 (1990).

⁴Yi Li, M. Farle, and K. Baberschke, *J. Magn. Magn. Mater.* **93**, 345 (1991); Yi Li and K. Baberschke, *Mater. Res. Soc. Symp. Proc.* (to be published).

⁵C. Rau, *J. Magn. Magn. Mater.* **31-34**, 874 (1983).

⁶A. Cerri, D. Mauri, and M. Landolt, *Phys. Rev. B* **27**, 6526 (1983).

⁷R. Bergholtz and U. Gradmann, *J. Magn. Magn. Mater.* **45**, 389 (1984).

⁸M. Farle and K. Baberschke, *Phys. Rev. Lett.* **58**, 511 (1987).

⁹G. H. J. Wentenaar, S. J. Campbell, D. H. Chaplin, T. J.

McKenna, and G. V. H. Wilson, *J. Phys. F* **9**, 935 (1979).

¹⁰G. H. J. Wentenaar, S. J. Campbell, D. H. Chaplin, T. J. McKenna, and G. V. H. Wilson, *Phys. Rev. B* **29**, 1419 (1984).

¹¹K. Baberschke, M. Farle, and M. Zomack, *Appl. Phys. A* **44**, 13 (1987).

¹²J. Kolaczkiwicz and E. Bauer, *Surf. Sci.* **175**, 487 (1986).

¹³D. Hull, *Introduction to Dislocations*, 2nd ed. (Pergamon, Oxford, 1975), p. 176.

¹⁴L. Hartshorn, *J. Sci. Instrum.* **2**, 145 (1925).

¹⁵F. H. Salas and M. Mirabal-Garcia, *J. Appl. Phys.* **66**, 5523 (1989). In this publication the experimental setup is presented at an early stage. At that time the sample preparation and the subtraction of the eddy current background could not be well reproduced and the temperature was not calibrated. Now χ_{ac} and T are absolutely calibrated. Primary field and frequency are stabilized to better than 10^{-5} .

¹⁶F. H. Salas and M. Mirabal-Garcia, *Phys. Rev. B* **41**, 10859

- (1990).
- ¹⁷N. Herzum, K. Stierstadt, and L. Wunsch, *Phys. Status Solidi (a)* **21**, 529 (1974).
- ¹⁸F. H. Salas, *J. Phys. C* **3**, 2839 (1991). We believe that the interpretation of the decrease in the signal at T_c as a first-order phase transition is dubious. The effect (Fig. 1) can be explained by the dominant background signal due to huge domain wall contributions, as can be seen from the dramatic differences in the two experiments. The data of Ref. 18 shows $\chi_{\text{wall}} \gg \chi_{\text{para}}$.
- ¹⁹For a review, see K. Stierstadt, R. Anders, and W. v. Horsten, *Phys. Daten 20-1* (Fachinformationszentrum, Karlsruhe, Germany, 1984), p. 68.
- ²⁰A. R. Chowdhury, G. S. Collins, and C. Hohenemser, *Phys. Rev. B* **33**, 6231 (1986).
- ²¹P. Sheng, C. B. Manikopoulos, and T. R. Carver, *Phys. Rev. Lett.* **30**, 234 (1973).
- ²²P. P. Freitas and J. B. Sausa, *J. Phys. F* **13**, 1245 (1983).
- ²³M. Vincentini-Missoni, R. I. Joseph, M. S. Green, and J. M. L. Sengers, *Phys. Rev. B* **1**, 2312 (1970).
- ²⁴J. C. LeGuillou and J. Zinn-Justin, *Phys. Rev. Lett.* **39**, 95 (1977).
- ²⁵D. J. W. Geldart, P. Hargraves, N. M. Fujiki, and R. A. Dunlap, *Phys. Rev. Lett.* **62**, 2728 (1989).
- ²⁶G. A. Baker, *Phys. Rev.* **124**, 768 (1961).
- ²⁷D. S. Ritchie and M. S. Fisher, *Phys. Rev. B* **5**, 2668 (1972).
- ²⁸K. R. Sydney, D. H. Chaplin, and G. V. H. Wilson, *J. Magn. Mater.* **2**, 345 (1976).
- ²⁹P. Hargraves, R. A. Dunlap, D. J. W. Geldart, and S. P. Ritcey, *Phys. Rev. B* **38**, 2862 (1988).
- ³⁰C. M. Soukoulis, G. S. Grest, and M. Velgakis, *Phys. Rev. B* **40**, 467 (1989).